Q. J. R. Meteorol. Soc. (1992), **118**, pp. 51–70 551.513.1:551.515.527:551.557.5 (265)

A GCM case study on the maintenance of short-term subtropical wind maxima in the summer hemisphere during SOP-1, FGGE

By JAMES W. HURRELL

National Center for Atmospheric Research, P.O. Box* 3000, *Boulder, Colorado* 80307

and

DAYTON G. VINCENT

Department of Earth and Atmospheric Sciences, Purdue University, West Lafayette, Indiana 47907

(Received 12 December 1990; revised 16 August 1991)

SUMMARY

A recent version of the GLA fourth-order GCM is used to investigate the short-term relationship between tropical heating and upper tropospheric subtropical westerly maxima in the summer hemisphere. Emphasis is focused on a 15-day forecast of the circulation corresponding to 6–20 January 1979. During this time, observational data from the FGGE suggested that strong convection over the South Pacific was helping to maintain a nearby subtropical jet. The dominant term in the zonal momentum budget was the Coriolis force applied to the diabatically driven meridional circulation, although the mean advection of zonal momentum and transient eddy momentum and sensible-heat transports made important contributions. A 'full-physics' forecast made with the GCM is able to simulate these processes to a reasonable degree of accuracy.

To examine the impact of direct meridional overturning on the rotational flow in the South Pacific, the latent energy supplied to the model atmosphere is reduced in two ways. First, negative sea-surface-temperature anomalies are imposed in the area of maximum convection. Second, temperature changes resulting from precipitation processes are ignored in the model thermodynamic equation. Results from both types of experiments are consistent, and they substantiate our earlier observational findings that, at least for this case study, summertime subtropical westerly maxima are largely forced by divergent outflow from the tropics.

1. INTRODUCTION

Recently the authors diagnosed pronounced short-term deviations in southern hemisphere (SH) tropical convection during the first Special Observing Period (SOP-1) of the First (GARP) Global Experiment (FGGE), 5 January–4 March 1979 (Hurrell and Vincent 1990, 1991, hereafter referred to as HV90, HV91). We were able to relate enhancements of divergent outflow from tropical heat sources to nearly instantaneous (less than 12-hour temporal resolution of the data) increases in the summertime subtropical zonal wind field, a type of circulation problem not well examined before. Most previous studies, many of which are summarized in HV90, have examined winter hemisphere interactions where the upper branch of the Hadley circulation is best defined and the subtropical westerly jet cores are much stronger. As shown in HV90 and Vincent *et al.* (1991), however, subtropical jet streaks are common in the summer hemisphere and, therefore, the more subtle forcing of these wind maxima is an equally important subject that needs to be addressed. It is the purpose of this paper to substantiate our earlier work by numerically testing the hypothesis that the observed summertime subtropical wind maxima were strengthened by episodes of enhanced tropical divergence. This will be accomplished through a series of experiments performed with a recent version of the Goddard Laboratory for Atmospheres (GLA) fourth-order general circulation model (GCM). Before describing the formulation and results of these experiments, however, it is relevant to summarize briefly the major findings presented in HV90 and HV91.

The major changes in tropical convection during the SOP-1 of the FGGE were first discussed by Paegle *et al.* (1983). They qualitatively related changes in heating that

* The National Center for Atmospheric Research is sponsored by the National Science Foundation.

occurred between January and February 1979 to the corresponding redistribution of zonal wind maxima in the northern hemisphere (NH). Examining similar time intervals, HV90 and HV91 used GLA Level III-b analyses to study the mean state of two 15-day periods, namely 6–20 January (Period 1) and 3–17 February (Period 2), that captured major changes in both the SH tropical heating and subtropical wind fields, especially over the South Pacific and Indian Oceans. In general, convection in the South Pacific convergence zone (SPCZ) was very strong during Period 1, and convective activity over the Indian Ocean increased during Period 2. Moreover, the corresponding changes in the meridional component of the tropical divergent wind (v_χ) were highly correlated to changes in the subtropical zonal wind fields. Maximum values of v_χ, which accounted for nearly all of the total ageostrophic meridional wind (v_a) in the SH subtropics and represented large accelerations by the Coriolis force, were located near the entrance regions of the maximum westerlies. In the NH, however, maxima of v_χ were at lower latitudes and the primary components of v_a in the stronger wintertime jet regions were rotational (Blackburn 1985; Trenberth and Chen 1988).

The relationship between the zonal wind component (u) and v_χ at 200 mb is shown for both 15-day periods, as well as their difference (Period 2 – Period 1), in Figs. 1 and 2. Even a cursory examination of the difference maps (Figs. 1(c) and 2(c)) gives evidence that the SH subtropical westerly maxima are closely related to regions of maximum poleward-moving divergent air. In particular, significant decreases in v_χ over the South Pacific and the coast of Brazil by Period 2 are tied to reductions in the westerlies in those areas. Conversely, increased poleward divergent flow between Australia and New Zealand and over the western Indian Ocean are highly correlated to enhanced westerlies in those regions.

The evidence from our observational studies supports the view that tropical heating in transient events enhances local meridional overturning which strengthens the summer subtropical westerlies. As stated earlier, it is the purpose of this study to substantiate the findings of HV90 and HV91 and, with the use of a recent version of the GLA GCM, further examine the extent to which the subtropical westerlies were influenced by divergent circulations. In essence, if medium-range forecasts with the model can reproduce the general features of the observed circulation, especially those which correspond to heating in the SH tropics and wind distribution in the subtropics, then the model becomes a mechanistic tool to study the extent to which the observed jet streams were enhanced by direct local meridional overturning. The formulation of the GCM will be briefly described in section 2, and the design and results from the control and experimental integrations will be described in section 3. Section 4 will present a summary and conclusions.

Before proceeding, however, it should be noted that the general approach taken with the numerical aspects of this work follows from the earlier work of Kalnay *et al.* (1986), Mo *et al.* (1987) and Nogues-Paegle and Mo (1988). They used a version of the GLA GCM similar to the one used here and performed medium-range integrations of approximately two-weeks' duration to study tropical/extratropical interactions. Of particular relevance to the present study is the paper by Nogues-Paegle and Mo. They initialized the model with real data and examined the transient response of the SH subtropical jet to tropical forcing during the 1979 SH winter season. For the period 25 July through 12 August 1979, Nogues-Paegle and Mo noted that observed accelerations of the 200 mb zonal wind over Australia between 25°S and 35°S were well correlated to enhanced area-averaged rainfall rates in the NH tropics at similar longitudes. Specifically, the enhancement episode culminated on 8 August with a zonal wind over Australia of 93 m s^{-1}. Consequently, they performed an integration, initialized on 1 August 1979, and

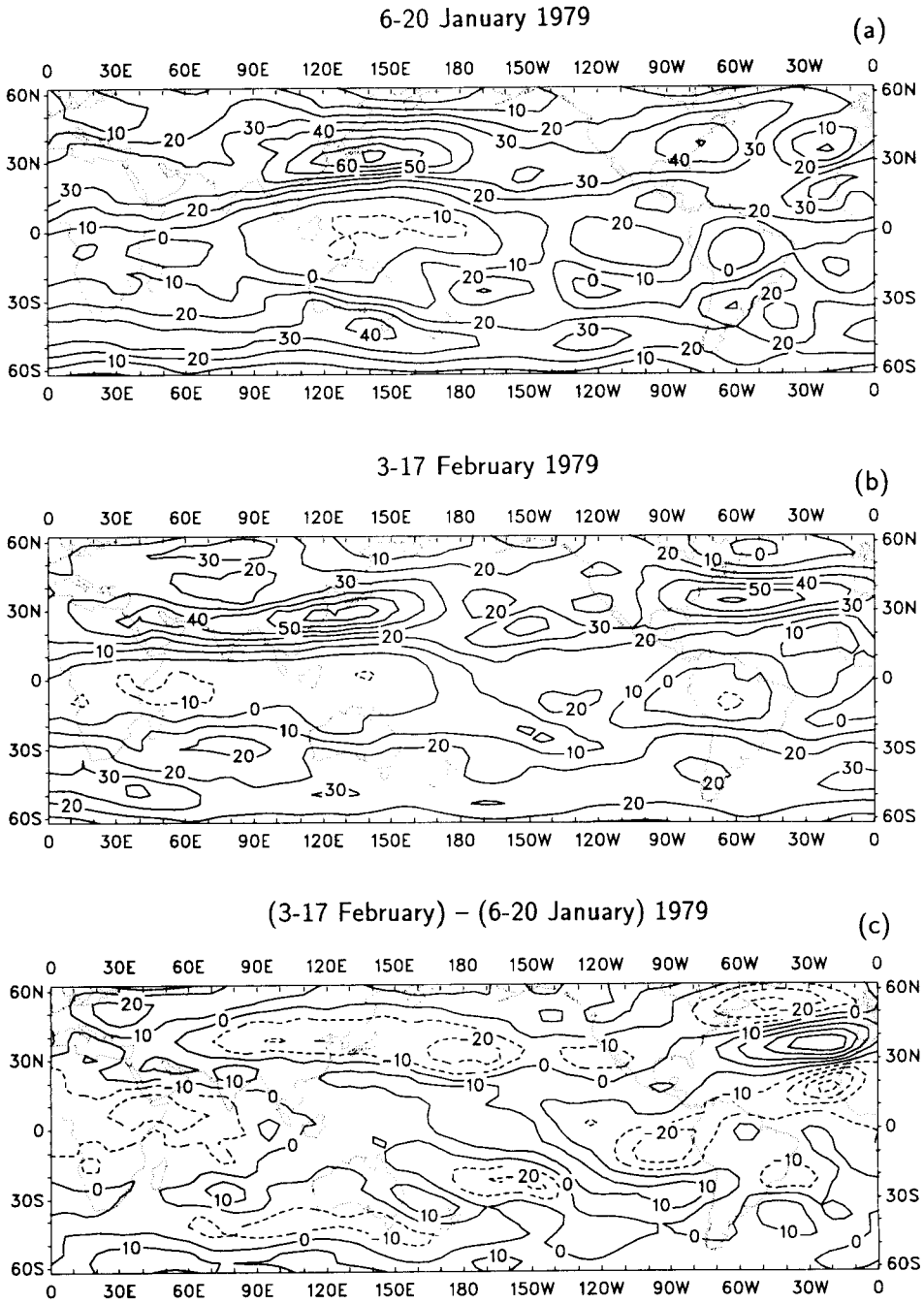

Figure 1. Zonal wind component at 200 mb for (a) 6–20 January 1979, (b) 3–17 February 1979 and (c) their difference. Contour interval is 10 m s^{-1} and negative values are dashed.

were able to reproduce a peak 200 mb zonal wind of 82 m s^{-1} during 8 August centred over Australia at about 26°S. Moreover, this zonal wind maximum corresponded favourably with increased upper-level divergent flow near 6°N, about 50° longitude upstream of the jet during 4 August. Since the control run was successful at simulating the temporal

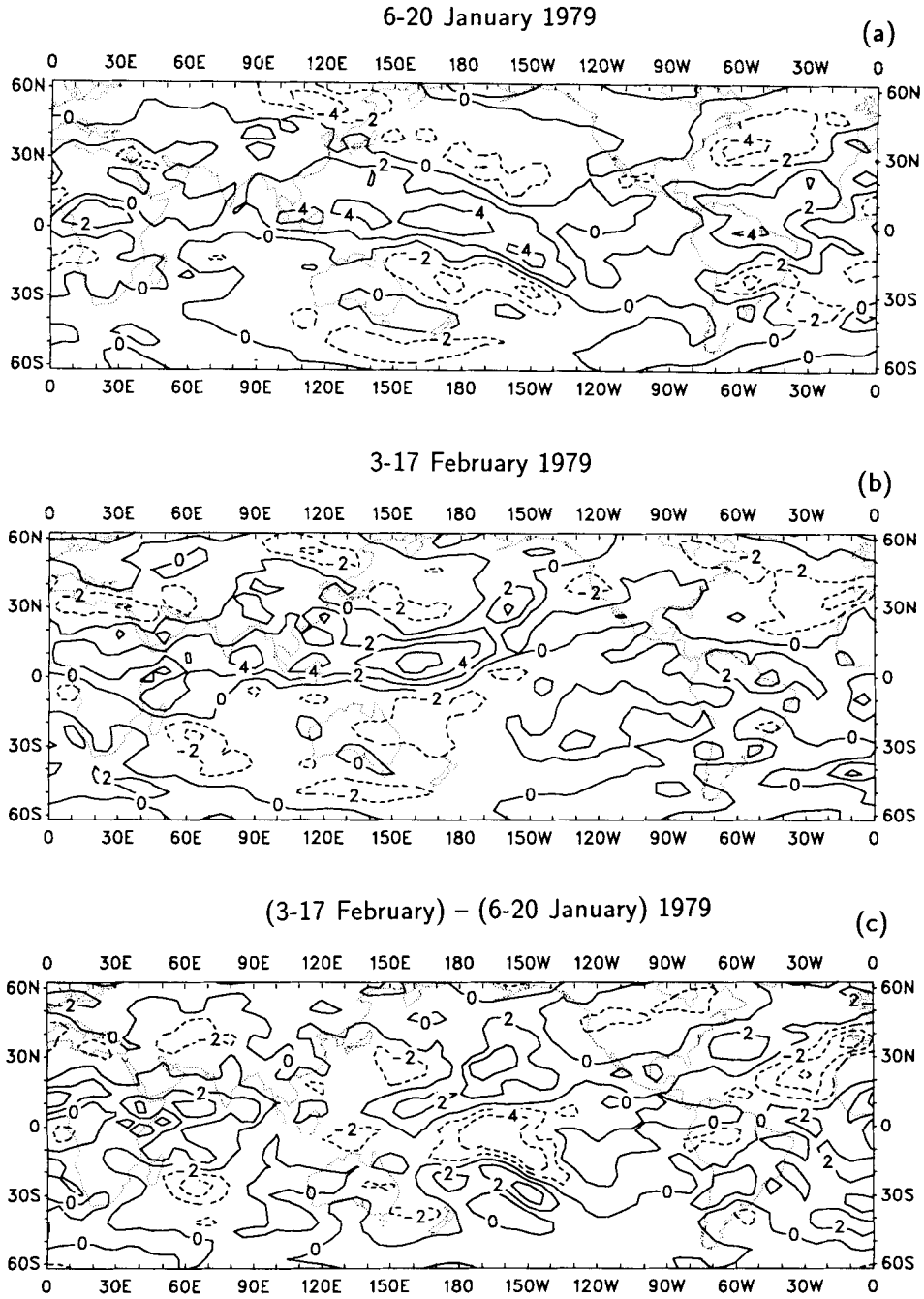

Figure 2. Meridional component of the divergent wind at 200 mb for (a) 6–20 January 1979, (b) 3–17 February 1979 and (c) their difference. Contour interval is 2 m s^{-1} and negative values are dashed.

and spatial evolution of the Australian wind maximum, they performed a numerical simulation with suppressed heating over the tropical Pacific from 90°E to 120°W. They found that the impact of the decreased latent-heat release was remotely felt at the wintertime subtropical latitudes in 2 to 4 days, and the result was a decrease of the subtropical jet over Australia to 61 m s^{-1} by 8 August.

2. Model formulation

The GLA fourth-order GCM has been successfully used in many forecast and general circulation experiments using the FGGE data (e.g. Paegle and Baker 1983; Kalnay *et al.* 1986; Mo *et al.* 1987; Nogues-Paegle and Mo 1988). The results of these studies have shown that the model is capable of producing accurate short- and medium-range forecasts (i.e. out to two weeks), as well as reproducing the climatological structure and seasonal variability of the general circulation with an accuracy comparable with the GCMs used at other facilities (Kalnay *et al.* 1983). By far the most complete description of the horizontal and vertical structure of the model, the governing equations and hydrodynamics, and many of the parametrized physical processes is given by Kalnay *et al.* (1983). More recently, however, several improvements have been made to the version of the model used in the aforementioned studies, especially with regard to the parametrization of cumulus convection. Many of these changes were implemented and are documented in detail by Sud and Molod (1988), and it is their version of the GCM which is used in the present study. Consequently, much of the following discussion is summarized from their work.

The basic structure of the model consists of a 4° latitude by 5° longitude uniform non-staggered horizontal grid and a generalized pressure coordinate system (sigma coordinates) to define nine layers of equal thickness in the vertical. The six prognostic variables contained within the model are the zonal and meridional winds, temperature and specific humidity of the nine sigma layers in the free atmosphere, as well as the surface pressure and ground temperature. The governing equations for these variables are written in spherical coordinates in flux form. They are solved in space using a quadratic energy-conserving scheme with horizontal differences computed to fourth-order accuracy, and the Matsuno (1966) scheme is used for integration in time.

The parametrizations of physical processes have evolved from the original version of the model described by Somerville *et al.* (1974). Details of many improvements are given by Kalnay *et al.* (1983) and include the planetary boundary-layer parametrization of Sud and Abeles (1980) and the parametrization of long-wave radiation by Wu (1980). More recent improvements include new parametrizations for dry convective adjustment, moist convective processes and cloud–radiation interaction implemented by Sud and Molod (1988). Since they give an excellent review of all the major physical parametrizations within the GCM, including a detailed discussion of their implementation of an Arakawa–Schubert-type cloud scheme and an improved rain–evaporation parametrization, it is not necessary to repeat their summary here. It is relevant to note, however, that the version of the model used in this study corresponds to the 'A6' version of Sud and Molod. We compared some of our results from medium-range (17-day) January 1979 integrations between the version of the model described by Kalnay *et al.* (1983) and the 'A6' version, and found that the 'A6' version gave more realistic distributions of both large-scale and convective clouds, precipitation patterns, and especially upper-level divergence fields throughout the tropics. Sud and Molod (1988) report similar findings for simulations of the July climatology. Obviously, this is an important improvement for the present study.

3. Model results

To test the ability of the GLA GCM to capture the major changes in the tropical heating and subtropical zonal wind fields between January and February 1979, 'full-physics' control integrations were performed for both of the 15-day observational periods

described earlier and in HV90 and HV91 (i.e. 6–20 January and 3–17 February). Daily time-interpolated boundary conditions of sea surface temperature (s.s.t.), snow and ice cover, albedo and soil moisture were obtained from monthly mean climatological values (see Volume 1, Appendix D of Kalnay *et al.* (1983) for the monthly mean distributions). Climatological s.s.t. was used since observed s.s.t. anomalies (not shown) were small (generally less than 0.5 deg C) over the tropical western Pacific during Period 1 and tropical Indian Ocean during Period 2. Initial conditions for these runs, as well as for the experiments to be described shortly, were obtained from GLA FGGE Level III-b global analyses. Specifically, 6–20 January (3–17 February) integrations were initialized with 0000 GMT 4 January (0000 GMT 1 February) GLA analyses. All runs were then integrated out to 17 days, but the first 2 days of the integrations were not considered in any subsequent averages in order to allow the model sufficient time to adjust to the initial conditions. The adjustment time of the model was determined through a comparison of 12-hour globally averaged values of evaporation and precipitation. It was found in both cases that the model evaporation and precipitation reached a close balance within the first 36 hours of each run. Thus, by eliminating the first 2 days, 15-day averages of model fields from the control runs were temporally consistent with the observational Period 1 and Period 2 results of HV90 and HV91.

In general, results from the Period 1 and Period 2 control integrations compared favourably with the observational results. The relationship between the upper tropospheric outflow and the subtropical westerly maximum over the Indian Ocean during Period 2, however, was not as well defined as that over the South Pacific during Period 1 in either the control integration or the observations. For this reason, and for brevity, only results from the Period 1 control integration will be presented. This allows us to focus attention on tropical/extratropical interactions over the South Pacific, a region of importance to global-scale circulations.

(*a*) *Control forecast*

Results from the Period 1 full-model-physics control integration, hereafter referred to as CNTRL, are illustrated in Fig. 3. Only the most relevant variables are presented, and the following discussion will be restricted to the mean state. Again, recall that only the last 15-days (6–20 January) of CNTRL have been averaged.

One diagnostic model quantity not directly available in the observational data is the total diabatic-heating rate (Q). A vertical profile of Q area-averaged over the tropics (not shown) revealed that the maximum heating in the model atmosphere occurred in the 400–500 mb layer. For this reason, the total diabatic heating at 500 mb from CNTRL is shown in Fig. 3(a). Values of $Q \geq 4$ K day^{-1} have been shaded to indicate regions of maximum convective activity. It is apparent that the strongest heating occurs over the Indonesian and SPCZ regions. This is in good spatial agreement with the lowest values of observed outgoing long-wave radiation (o.l.r.) in the tropics for January 1979 (Fig. 1(a) in HV90). Elsewhere, large heating rates are seen in CNTRL near the equator over South America and Africa, again in agreement with observed convective activity noted over the continents in HV90. The heating over the Indian Ocean is probably too strong and extensive in CNTRL, although low values of observed o.l.r. were noted just north of Madagascar.

A vector plot of the total 200 mb divergent wind field ($\mathbf{v}_\chi$) from CNTRL overlayed on a contoured map of the rotational zonal wind, u_ψ, is presented in Fig. 3(b). For reference, note that the maximum divergent wind speed (indicated by the length of the maximum vector) is 7.5 m s^{-1}. As in the observations (see Fig. 1 of HV91), the strongest outflow in the SH tropics is from the Indonesian and SPCZ regions, and the largest

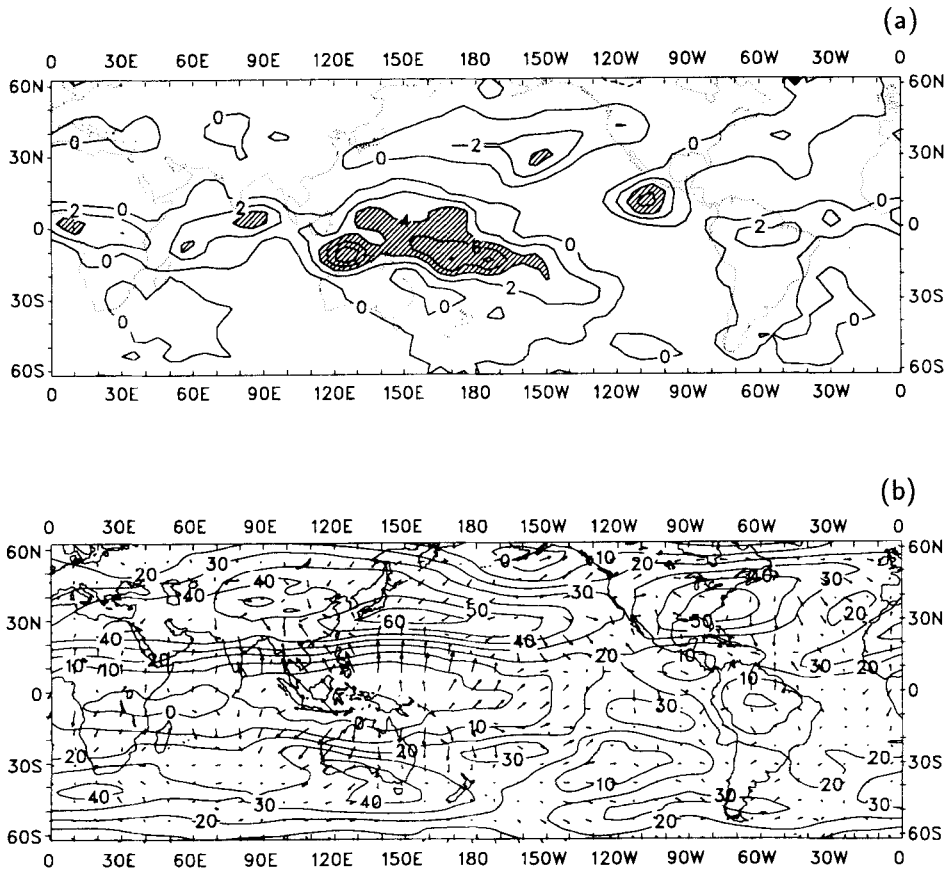

Figure 3. Period 1 CNTRL results for (a) total diabatic-heating rate at 500 mb and (b) vector plot of the divergent wind overlayed on a contoured plot of the rotational zonal wind at 200 mb. Contour interval in (a) is 2 K day^{-1} and in (b) is 10 m s^{-1}.

values of $\mathbf{v}_\chi$ are found at low latitudes in the NH south of the maximum westerlies. Of greatest relevance to the present study is the simulation of strong meridional outflow into the SH subtropics and especially into the entrance region of a westerly maximum near the east of the International Date Line (IDL). The most notable difference in $\mathbf{v}_\chi$ between the observations and CNTRL is that the simulated meridional outflow over Australia and the Indian Ocean is too strong, while that over the central South Pacific and south-east Brazil is too weak. In spite of these differences, however, the results from CNTRL are very encouraging. The most relevant point is that the sign of the meridional divergent wind, v_χ, agrees nearly everywhere with the observations, and the regions of maximum meridional divergent flow are the same as in Fig. 2(a), even though the magnitudes do not agree exactly. Furthermore, CNTRL captures the relationship between v_χ and the subtropical zonal winds evident in the observations. This point is now addressed further.

The rotational component of the zonal wind is shown in Fig. 3(b), as opposed to the total u-wind presented in Fig. 1, since the explicit purpose of the experimental runs (to be described shortly) is to alter the divergent circulations in the regions of the subtropical westerly maxima. This presents no major inconsistency with the observational results since the subtropical jet cores evident in the observational data are nearly totally

depicted by the rotational flow (HV91). A comparison of Fig. 3(b) with Fig. 1(a) shows good agreement around the globe, although the zonal wind is approximately 5 m s^{-1} too strong nearly everywhere in CNTRL compared with the observations. The SPCZ westerly maximum is clearly evident in CNTRL, as is the westerly jet south of the equator over the eastern Pacific. Both of these wind maxima are separate from the higher-latitude SH jet stream, which was also the case in the observations. The tropical westerly maximum over the eastern Pacific is a particularly interesting feature. The existence of a westerly flow region of limited zonal extent over the eastern tropical Pacific Ocean at 200 mb has also been noted in the seasonal data of Newell *et al.* (1972) and Sadler (1975). Webster and Holton (1982), using a shallow-water model, have pointed to the existence of this westerly 'duct' as representing a corridor for cross-equatorial interactions. Elsewhere, easterlies are present over the regions of strongest tropical heating in CNTRL, and, in the winter hemisphere, the strong jet cores over the east coasts of Asia and North America are successfully reproduced.

A more thorough evaluation of CNTRL can be gathered from a comparison with observations of individual terms in the zonal momentum equation. The tool utilized here is the transformed time-mean Eliassen–Palm (E–P) flux zonal momentum equation developed by Trenberth (1986) and presented and discussed in HV91 (Eq. (8)). Only the forcing terms most important to the local momentum balance in the western and central tropical and subtropical Pacific are presented in Fig. 4 for the observations and Fig. 5 for CNTRL. These terms represent accelerations of the zonal wind by the Coriolis force applied to the diabatically driven divergent meridional wind (top panels), the net impact of eddy momentum and sensible-heat transports (middle panels), and the 3-dimensional mean advection of zonal momentum (lower panels). Each term has been multiplied by $\cos\phi$ so that the results in Figs. 4 and 5 apply to tendencies in $u\cos\phi$.

The top two panels in Fig. 4 were presented in HV91 for a more limited region and differ only slightly as a result of a weak smoothing applied to the current results. The Coriolis term (Fig. 4(a)) is responsible for a strong acceleration of the westerlies in the SPCZ jet entrance region, and positive accelerations are evident in all regions where the meridional divergent wind (see Fig. 3(b)) is directed poleward. The total E–P flux divergence is given in Fig. 4(b) and represents the net effect of transient eddies. Their impact is to partially offset the strong Coriolis acceleration in the SPCZ jet entrance region through momentum flux divergence, while near the exit region (26°S, 160°W) they help accelerate the jet. Thus, it appears the net effect of transient eddies in the SPCZ region is to move the local jet eastward. The mean advection term (Fig. 4(c)) also acts to move the SPCZ jet eastward, and appears as the dominant term in the momemtum budget near the higher-latitude westerly maximum just south of Australia. These results for the Period 1 observations are discussed in more detail in HV91. As noted there, the magnitudes of the terms in Fig. 4 should be interpreted with caution, since errors and uncertainties in the observational analyses are magnified when divergences are computed. While a general balance exists, the sum of the terms in Fig. 4, and the smaller forcing terms not presented, sometimes shows large imbalances which may well reflect analysis uncertainties. This point should be kept in mind during the following discussion.

Figure 5 serves to illustrate the agreement, as well as the disagreement, between CNTRL and the observations. As in Fig. 4(a), the Coriolis force is responsible for large accelerations in the entrance region of the SPCZ westerly maximum in CNTRL, and the axis of maximum values of v_χ is well simulated although the outflow is too strong. As noted previously, compared with the observations the meridional outflow is also too strong over and to the west of Australia, but it is too weak over the central South Pacific. This last fact points to the failure of CNTRL to reproduce accurately the strength of the

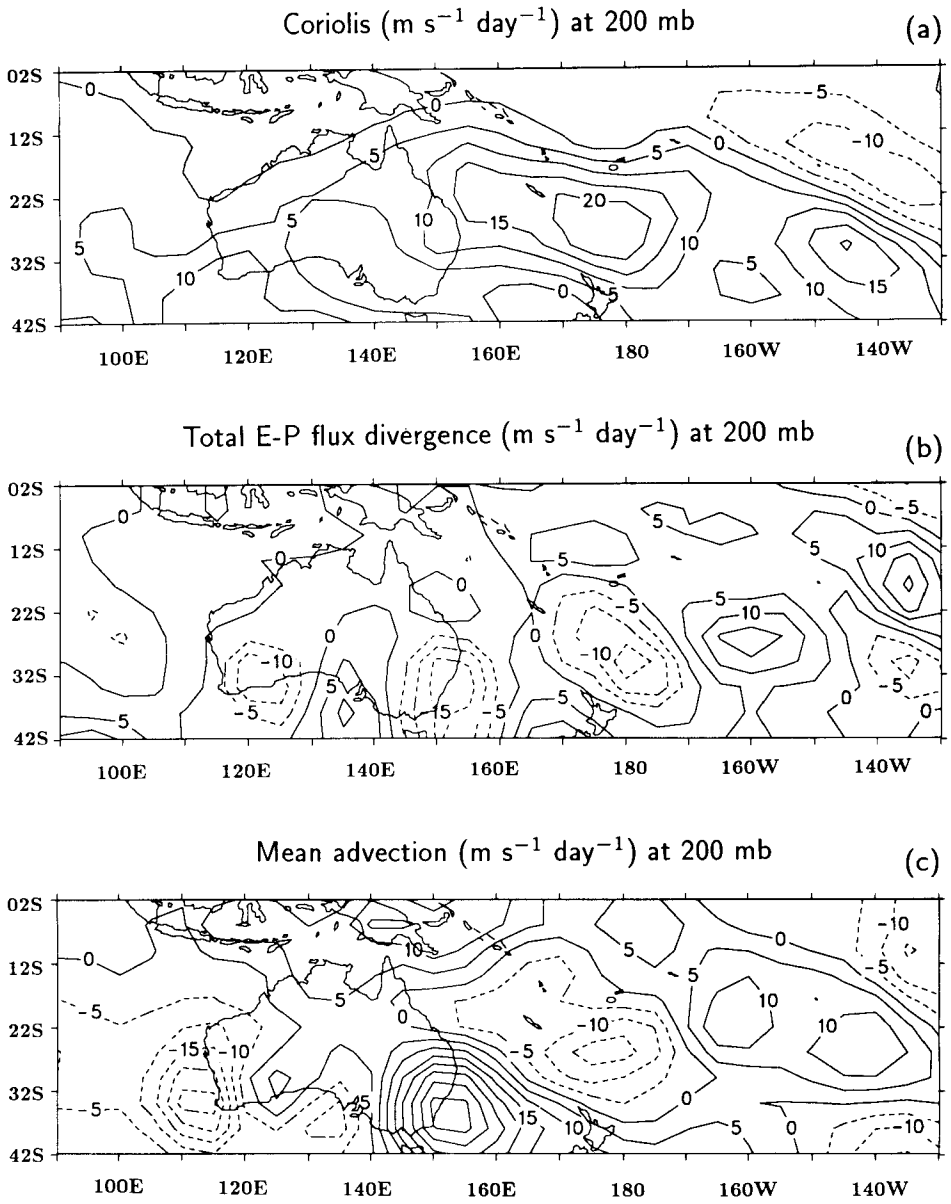

Figure 4. Acceleration of the zonal wind by (a) Coriolis term, (b) total zonal E–P flux divergence and (c) mean advection terms. All for 6–20 January 1970. Contour interval is 5 m s^{-1} day^{-1} and negative values are dashed.

north-west to south-east diagonal extension of the SPCZ. The total E–P flux divergence from CNTRL (Fig. 5(b)), as in the observational data, largely offsets the Coriolis term in the SPCZ jet entrance region and helps accelerate the westerlies near the exit. Again, the accelerations are larger than observed. The effect of eddy momentum and heat transports on the zonal wind is not as accurately simulated elsewhere, especially over south-west Australia and to the east and north of the SPCZ westerly maximum. The spatial pattern of accelerations by the mean advection of zonal momentum (Fig. 5(c)) generally agrees with the observed distribution, although the maximum values are often weaker and misplaced. For example, the negative tendencies in the SPCZ jet entrance

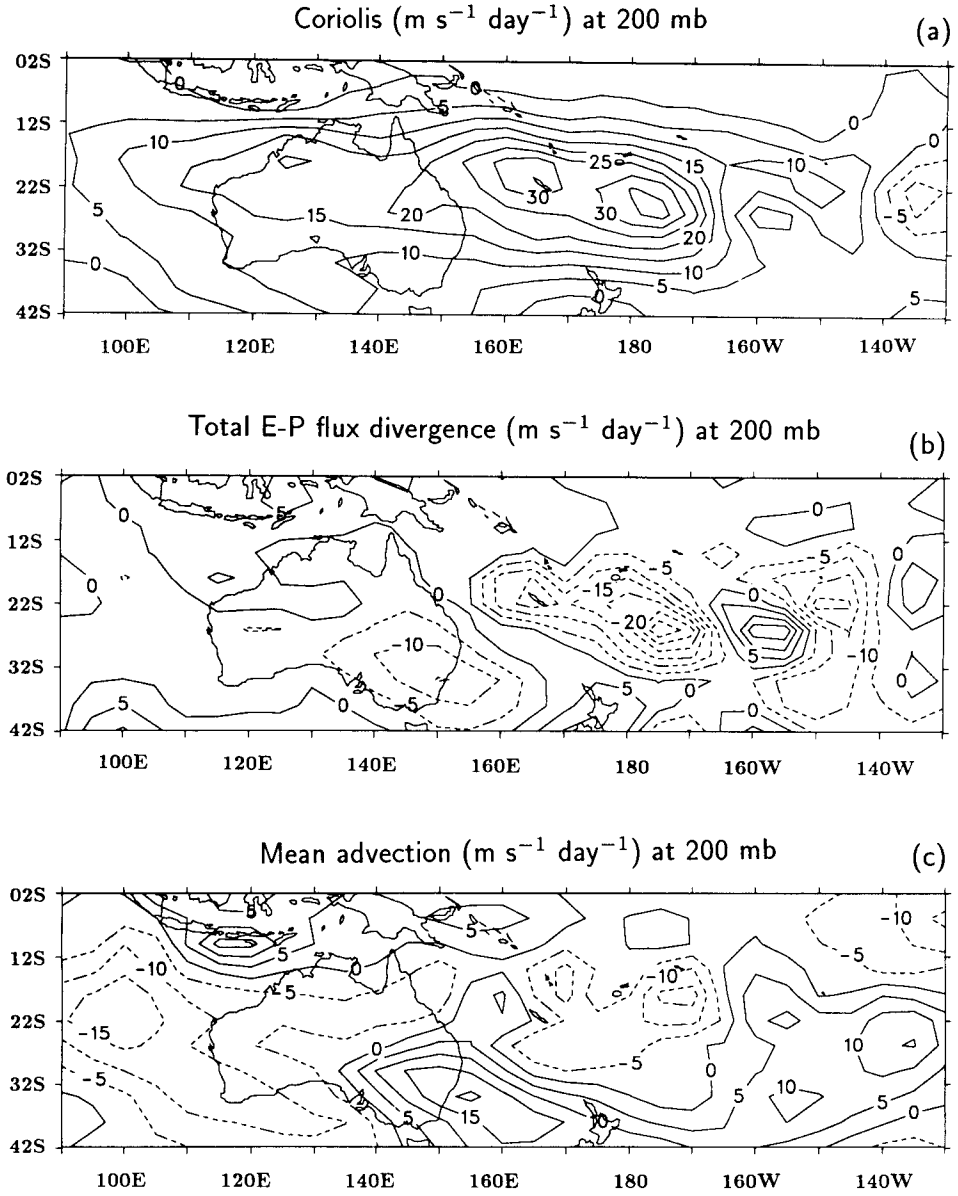

Figure 5. Acceleration of the zonal wind by (a) Coriolis term, (b) total zonal E–P flux divergence and (c) mean advection term for CNTRL. All at 200 mb. Contour interval is 5 m s^{-1} day^{-1} and negative values are dashed.

region in CNTRL are smaller than observed, and the positive tendencies just east of the subtropical jet south of Australia are nearly 50% too weak. These features primarily reflect a poor simulation of the observed westerly minimum over Australia. Consequently, the zonal and meridional gradients of u_ψ are too weak in CNTRL.

We conclude that CNTRL simulates the processes most important to the maintenance of the SPCZ westerly maximum during Period 1. Thus, we can now use the GLA GCM to examine the extent to which subtropical westerlies in the summer hemisphere are enhanced by direct local meridional overturning.

Before proceeding to the results of the experimental runs, however, the question arises as to whether the information necessary to simulate the observed circulation is contained primarily in the s.s.t. or the atmospheric initial conditions. Certainly, the correct specification of s.s.t. is important in order to maintain episodes of enhanced convective outflow in the GLA model, and again we emphasize that Period 1 observed s.s.t. was very similar to the model climatological values used in CNTRL. Moreover, it appears that SH summer subtropical westerly maxima are common in both the observations (HV90; Vincent *et al.* 1991) and in longer-range (45-day) integrations with the GLA GCM, and these wind maxima are most numerous and strongest when located just poleward of the maximum divergent outflow. We believe, therefore, that the version of the model used here is capable of simulating realistic tropical heating/subtropical wind relationships given a realistic s.s.t. distribution, but the simulation of a specific case study is most accurate given initial data that are representative of the atmosphere at that time. This is not to say, however, that the results of medium-range forecasts from the GLA GCM such as CNTRL are overly sensitive to the particular initial conditions specified. For example, the results of CNTRL varied little for 18-day and 16-day full-physics forecasts begun one day earlier and later, respectively. This is an important point to keep in mind since a question often asked in sensitivity experiments is whether or not detected changes are due to predictability error growth (Daley and Chervin 1985). This results as model integrations of slightly different initial conditions diverge from each other in time owing to system nonlinearities. Suffice it to say that differences between CNTRL and the 18-day and 16-day control forecasts (not shown) were much smaller than those between CNTRL and the sensitivity experiments to be described in the following sections. For this reason, it appears as though changes evident in the experimental-model results can realistically be attributed to changes made in the model physics, especially since the results make physical sense. However, rigorous statistical tests (e.g. Zwiers and Storch 1989) were not conducted to verify this claim. To evaluate adequately the model variability, and verify the significance of responses to changes made in the model physics, several control and sensitivity experiments with perturbed initial conditions needed to be performed. Unfortunately, it was not feasible to execute the number of integrations with the full GCM required to satisfy this goal.

(*b*) *Model experiments*

The hypothesis to be tested is that subtropical westerly maxima and, in particular, the SPCZ westerly maximum during Period 1 are enhanced by direct local meridional circulations. In this case, tropical heating produces upward motion which results in upper-level divergent cross-isobaric flow towards the entrance regions of the subtropical westerly maxima. The westerlies are then accelerated through the action of the Coriolis force. The possibility that a reduction in tropical heating will decrease the divergent meridional winds and will impact the acceleration of the subtropical wind maxima is examined through two different approaches. First, tropical heating is reduced through the imposition of negative s.s.t. anomalies. The results from this experiment will be presented in some detail. Second, temperature changes due to precipitation processes are ignored in the model thermodynamic equation.

(i) *s.s.t. anomaly experiments.* In order to reduce the latent energy supplied to the atmosphere over the local area of the SPCZ and western Pacific, we performed a series of three s.s.t. reduction experiments (described below) all beginning with the same initial conditions used in CNTRL. The mean s.s.t. field during Period 1 from CNTRL is illustrated in Fig. 6(a). This map represents the time-interpolated monthly mean cli-

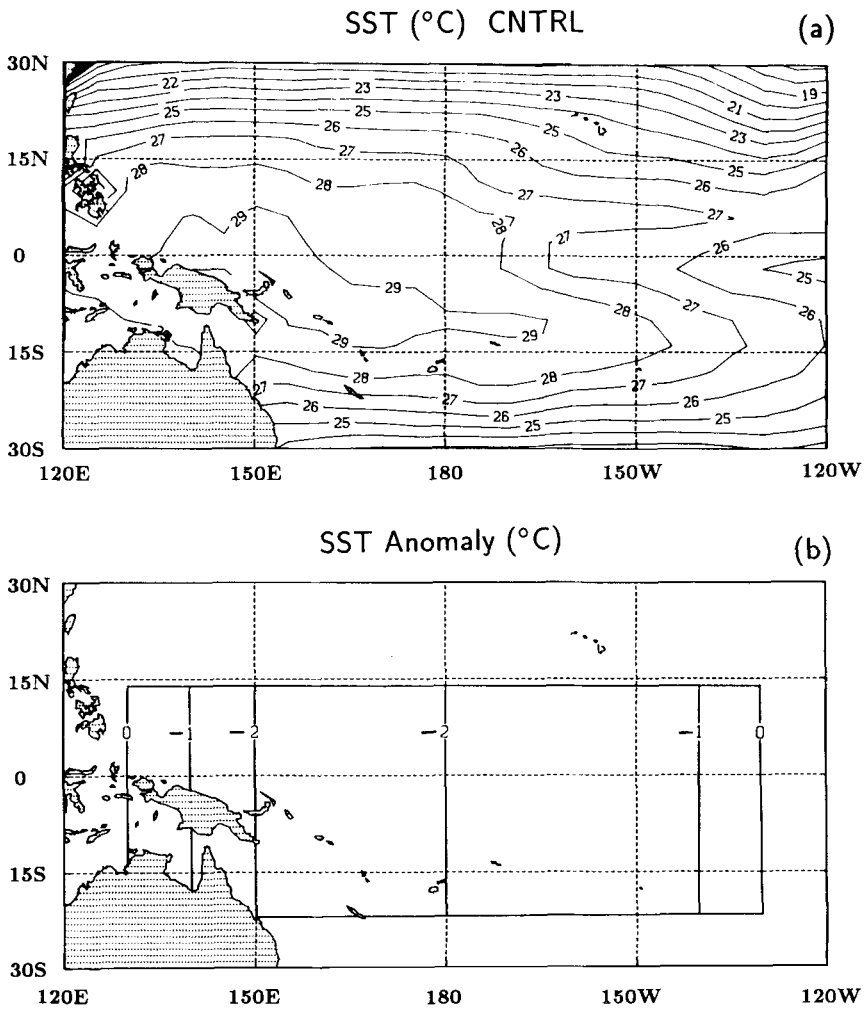

Figure 6. (a) Sea surface temperatures from CNTRL and (b) negative sea-surface-temperature anomalies imposed for SST1. Both for 6–20 January 1979. Contour interval is 1 deg C.

matological s.s.t. fields input into the model as boundary conditions. It is seen that model s.s.t.s in excess of 29°C are generally confined to the SH and extend from north of New Guinea south-east to 165°W. Furthermore, a comparison with Fig. 3(a) shows that the region of warmest s.s.t. corresponds well with the region of maximum 500 mb diabatic heating. This agrees with the finding of Storch *et al.* (1988) who illustrated that the tropical zonally oriented portion of the SPCZ is closely tied to relatively high s.s.t.s.

To diminish the strong heating and the resulting $\mathbf{v}_\chi$ field evident in Fig. 3(b), three different negative s.s.t. anomalies were imposed on the climatological s.s.t. fields over the western and central Pacific. The s.s.t. anomaly field for the first experiment (SST1) is given in Fig. 6(b). The input s.s.t. anomalies are confined to an area bounded by the latitudes of 14°N and 22°S, and extend from 130°E to 130°W. The largest reduction of 2 deg C is applied between 150°E and the IDL, which corresponds to the area of maximum heating and divergent outflow, as well as the entrance region of the SPCZ westerly maximum in CNTRL. Careful attention was given in the development of the s.s.t. anomaly field to reduce the strength of any artificially created s.s.t. gradients in either

the zonal or meridional directions. Kiladis *et al.* (1989) postulate that strong meridional s.s.t. gradients may help support convection in the diagonal portion of the SPCZ. The s.s.t. anomaly field shown in Fig. 6(b) remained constant throughout the integration, and it was made larger than observed anomalies over this region (for the time-scale used in the present study) so as to produce a signal which was clear enough to be distinguished from noise. With regard to this last point, the second and third s.s.t. experimental integrations (SST2 and SST3) consisted of imposed anomalies 1.5 and 2 times the anomaly used in SST1, respectively. These runs were produced to ensure an atmospheric response to the imposed anomalies on a time-scale of 15 days. As will be shown next, however, a clear response was found in the SST1 experiment, so the results of SST2 and SST3 will not be presented.

Figure 7 presents the same variables for the SST1 experiment as were shown for CNTRL (Fig. 3). Several large changes in the circulation are apparent. Most notable is the strong reduction of the 500 mb diabatic heating (Fig. 7(a)) over the western and central Pacific where only a small area of $Q \geq 4$ K day^{-1} is present east of the IDL near 10°S. As desired, the greatest changes from CNTRL are limited to the region of the imposed s.s.t. anomalies, although small differences do exist in the Q-field around the globe and include increases over the tropical Indian Ocean and South America. The changes in heating are reflected in the $\mathbf{v}_\chi$-field for SST1 presented in Fig. 7(b). In comparison with Fig. 3(b), the strong reduction in divergence over the western and

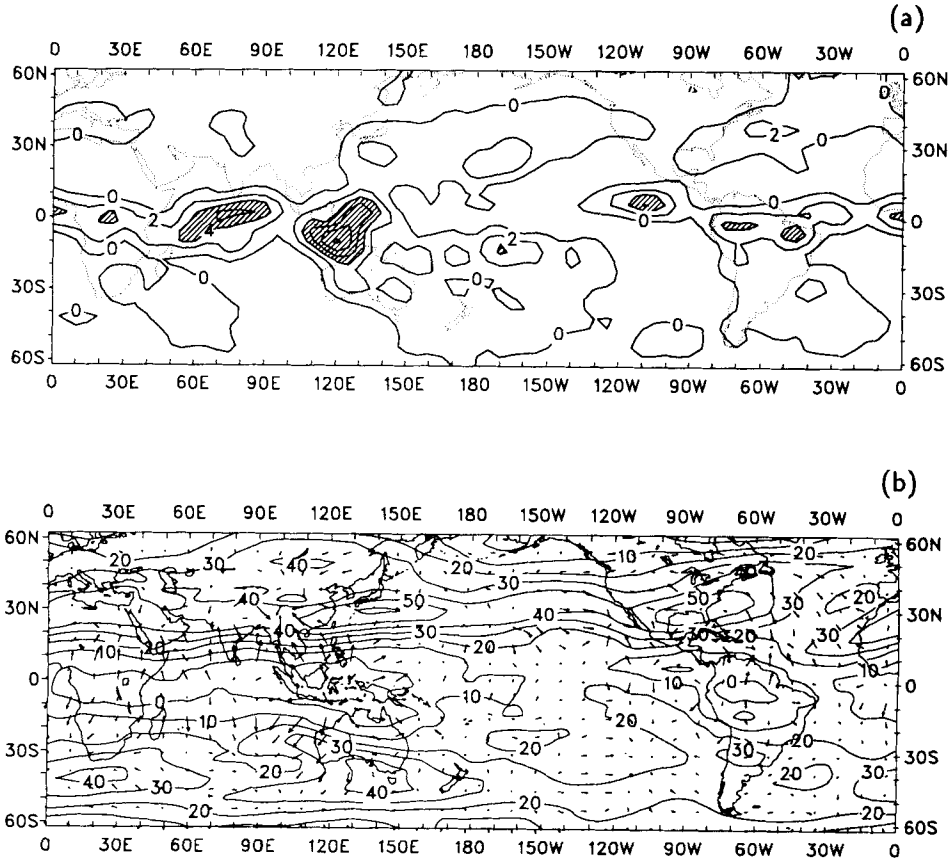

Figure 7. As Fig. 3 but from SST1.

central Pacific is clearly evident, while the divergent circulations elsewhere are minimally affected. Clear changes in u_ψ are also evident in Fig. 7(b), but variations from CNTRL are most easily seen in difference maps.

Differences between the CNTRL and SST1 divergent meridional wind fields are illustrated in Fig. 8(a). It is apparent that the strongest reductions in v_χ are local (i.e. over the western Pacific Ocean) and consist of decreases of poleward flow in both hemispheres in excess of 4 m s^{-1}. Changes elsewhere in the SH are very small, but several isolated regions of 2 m s^{-1} increases in v_χ extend from north-west to south-east across the North Pacific. The impact of the reduced heating and divergent circulations on the 200 mb rotational zonal wind field is shown in Fig. 8(b). As suggested by the observational results of HV90 and HV91, the mean-state SPCZ westerly maximum appears to be strongly influenced by the diabatically driven divergent outflow. In the entrance region of the SPCZ westerly maximum, which is located in an area of reduced v_χ and just poleward and eastward of the largest reductions, decreases of more than 10 m s^{-1} in u_ψ are observed in SST1. Smaller reductions are evident in the exit region of the jet where transient eddies make the dominant contribution to the balance of the time-mean momentum budget through eddy momentum flux convergence (Fig. 4(b)). It should be noted that the magnitude of the changes evident in Fig. 8(b) reflect the fact that the strength of the convection slowly decreased as the effect of the negative s.s.t. anomalies

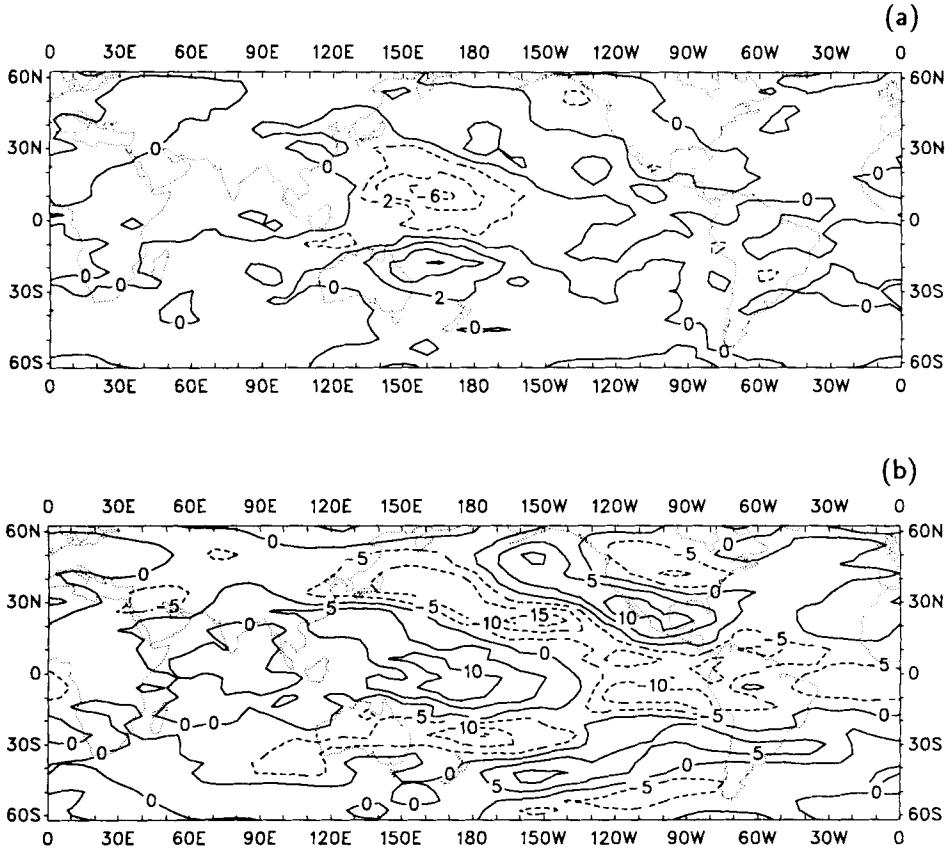

Figure 8. Differences at 200 mb between SST1 and CNTRL for (a) meridional component of the divergent wind and (b) zonal component of the rotational wind. Contour interval in (a) is 2 m s^{-1} and in (b) is 5 m s^{-1}. Negative values are dashed.

became more pronounced during the course of the integration. Some insight into the response time of the circulation to the imposed anomaly will be given shortly.

Outside of the subtropical western Pacific, where decreases in u_ψ can be directly attributed to reduced tropical divergence, changes in u_ψ appear to be part of a well-defined response evident in both hemispheres. Namely, the difference patterns in u_ψ appear to be consistent with the propagation of Rossby waves away from the region of maximum heating in CNTRL. Of coure, a confirmation of this response is not possible based solely on viewing the organized features evident in Fig. 8(b), and would require forcing a much simpler model with the CNTRL and SST1 divergence fields. Since this is not the purpose of this study, it is sufficient to say that the u_ψ response is consistent with the results of simpler model studies that have examined the extratropical response to tropical heating (e.g. Lau and Lim 1984; Sardeshmukh and Hoskins 1988).

From a momentum or kinetic-energy budget standpoint, the elongated u_ψ response is more difficult to assess. In the NH, increased (decreased) u_ψ tends to occur just to the east of increased (decreased) v_χ, although differences between CNTRL and SST1 in other forcing terms are not as uniform. This is also true in the SH, where an example is the u_ψ response over and to the west of Australia upstream from the reduced tropical heating. Differences between SST1 and CNTRL in the primary forcing terms in the E–P flux zonal-momentum equation are presented in Fig. 9 for the same limited region as before. As indicated by Fig. 8(a), reductions in the Coriolis term make the largest contribution to reduced westerlies from central Australia across the central Pacific. Just to the east of Australia, however, much of this reduction is counteracted by positive differences in the total E–P flux divergence and the mean advection terms, although the overall tendency remains negative. Over western Australia and the adjacent subtropical Indian Ocean, however, increases in the Coriolis term are smaller than the combined decreases in the transient-eddy and mean-advection terms. The point is that circulation changes in SST1 affect the momentum budget differently in different regions so that the elongated u_ψ response cannot be readily understood from changes in any one forcing term.

The response time of the divergent- and rotational-flow components to the imposed s.s.t. anomaly was examined through analyses of 12-hour model output (not shown). It was found that decreases in the divergent wind, and thus the impact of the s.s.t. anomalies on the forecast circulation, were first detected about 4 days into the integration. At all times, the response was essentially limited to the s.s.t. anomaly region. The response of the rotational zonal wind was initially limited to the SPCZ region as well, and changes in u_ψ evolved in phase with changes in v_χ; that is, decreases in u_ψ of about 5 m s^{-1} in the SPCZ region were also noted 4 days into the integration. After 10 January, decreases as large as 15 m s^{-1} were noted in the entrance region of the SPCZ jet, and changes resembling those seen in the mean-state difference map (Fig. 8(b)) were noticeable at higher latitudes and east of the western Pacific in both hemispheres.

(ii) *Reduced-tropical-heating experiments.* Another approach to examine the impact of tropical heating on subtropical rotational flows is to alter directly the temperature change due to precipitation processes in the thermodynamic equation. This approach has been more widely applied in investigations of this nature, especially in studies that have utilized the GLA GCM (e.g. Paegle and Baker 1983; Kalnay *et al.* 1986; Mo *et al.* 1987; Nogues-Paegle and Mo 1988). In this study it was decided to eliminate temperature changes in the model thermodynamic equation due to precipitation processes in a latitude belt from 18°S to 18°N over all longitudes. This includes latent-heat release due to both supersaturation and convective precipitation. For consistency, temperature changes due

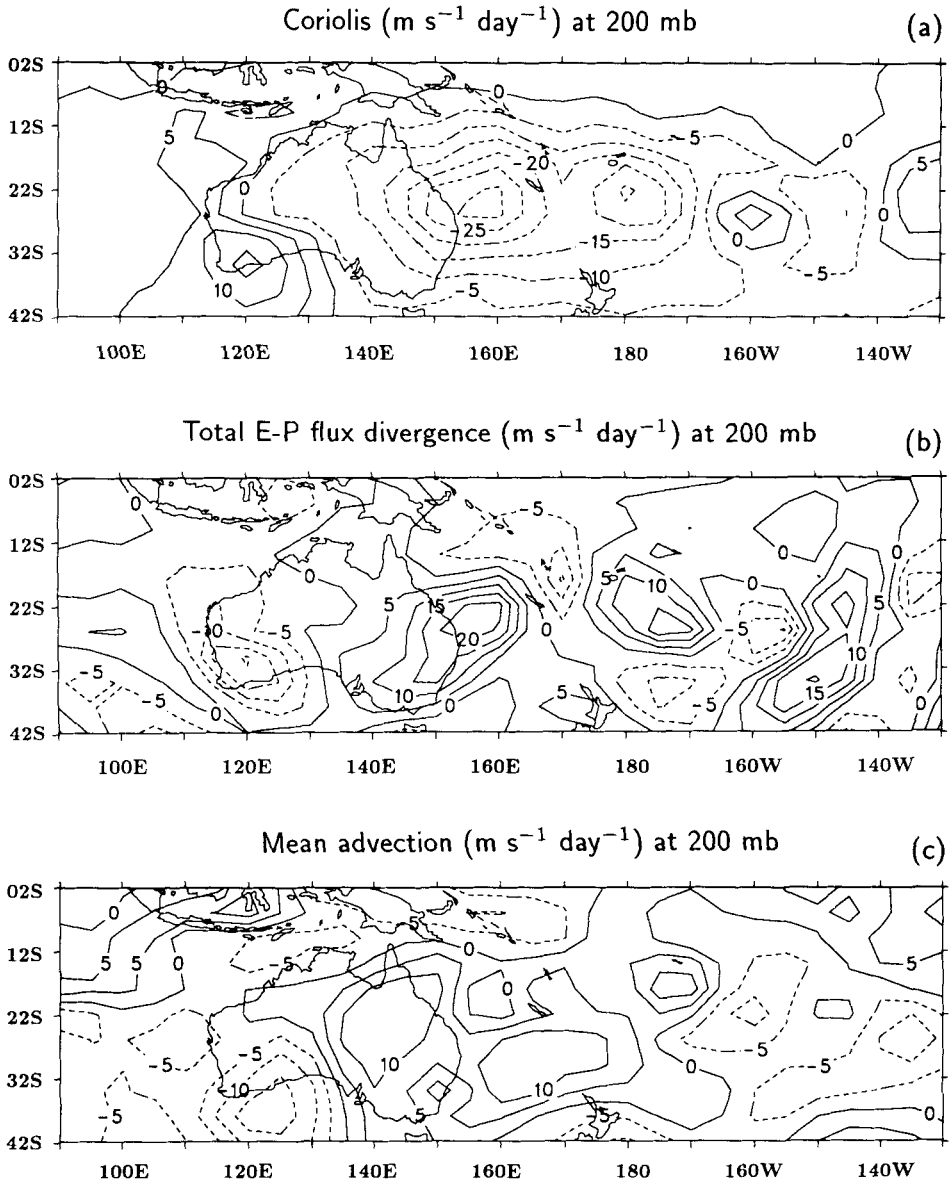

Figure 9. Differences at 200 mb between SST1 and CNTRL for accelerations of the zonal wind by (a) Coriolis term, (b) total zonal E–P flux divergence and (c) mean advection. Contour interval is 5 m s^{-1} day^{-1} and negative values are dashed.

to evaporation of falling precipitation were also neglected. The total suppression of these diabatic effects was gradually relaxed poleward of 18° latitude until the full impact of latent heating was felt at 30° latitude in both hemispheres. Otherwise, the model physics were unchanged from CNTRL.

The results from the no-tropical-latent-heating experiment, hereafter referred to as NTLH, showed major changes in the tropical belt at all longitudes. In particular, the 500 mb diabatic heating exhibited slight cooling throughout most of the tropics, in stark contrast to the strong heating evident in CNTRL. This cooling is in agreement with the results of a 5-day reduced-tropical-heating forecast experiment performed by Paegle and

Baker (1983) and, presumably, is a consequence of radiative cooling due to relatively enhanced infrared radiative flux divergence. As for SST1, the impact of the NTLH experiment on the divergent and rotational flows is most easily seen through difference maps.

The difference in v_χ at 200 mb between CNTRL and NTLH is illustrated in Fig. 10(a), and the difference in u_ψ is shown in Fig. 10(b). Unlike the localized impact seen in SST1, the approach of NTLH essentially eliminated the 200 mb divergence throughout the tropics; thus, Fig. 10(a) is nearly a reverse image of the v_χ field exhibited in CNTRL. Apparently, these strong changes in the divergent wind field are responsible for equally dramatic differences in the rotational zonal wind as well. It is seen from Fig. 10(b) that significant reductions of u_ψ occur throughout the subtropics, including maximum decreases in excess of 25 m s^{-1} in the vicinity of the SPCZ westerly maximum and in the regions of the climatological wintertime jet cores. The equality of the decreases in both hemispheres emphasizes, in relative terms, the importance of tropical heating to the maintenance of the weaker summertime subtropical westerly maxima (i.e. the thermal gradients in the SH subtropics are almost entirely eliminated). The fact that changes in u_ψ are stronger and more global than those in SST1 is merely because of the severity of the changes made to the model physics in NTLH.

It is interesting to contrast the time response of the divergent and rotational circulations in NTLH to those in SST1. Examinations of 12-hour model output fields

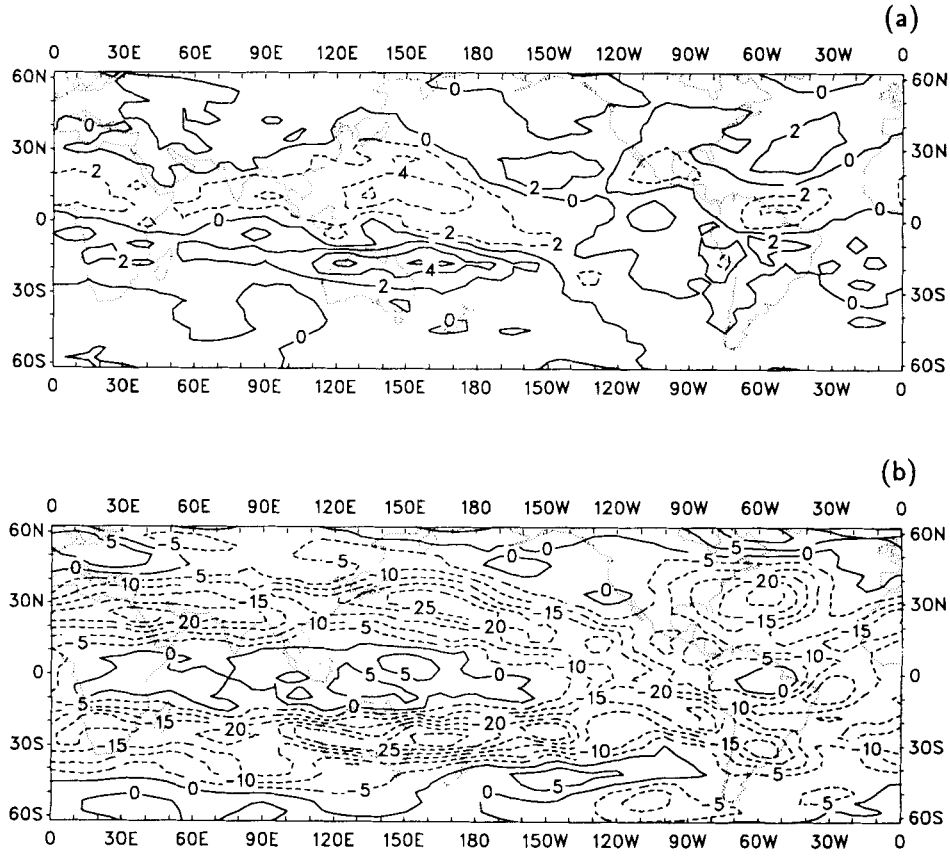

Figure 10. Differences at 200 mb between NTLH and CNTRL for (a) meridional component of the divergent wind and (b) zonal component of the rotational wind. Contour interval in (a) is 2 m s^{-1} and in (b) is 5 m s^{-1}. Negative values are dashed.

(not shown) revealed that, unlike SST1, the divergent circulations reacted to the reduced tropical latent heating within half a day of the beginning of the experiment. This same result was also found by Paegle and Baker (1983). Apparently, this time response indicates that the divergent wind is adjusted by rapidly propagating gravity waves and may, therefore, be quickly modified by changes in tropical heating (Paegle 1978; Paegle *et al.* 1983; Nogues-Paegle and Mo 1988). Indeed, Silva-Dias and Paegle (1984) illustrated that during the northern winter season of the FGGE most of the tropical divergence field projected on the gravity waves of a normal mode decomposition, and only a small fraction projected upon rotational modes.

The response of the rotational wind in the SH subtropics, and in the SPCZ region in particular, appeared to be in phase with changes in v_χ; that is, the response was almost immediate. Outside of the SH subtropics, however, the impact of the reduced latent heating was felt in u_ψ approximately 2–3 days after the beginning of the experiment, in good agreement with the results of Paegle and Baker (1983) and Nogues-Paegle and Mo (1988). The more immediate response of the rotational flow in the summer subtropical belt might be a result of the asymmetric distribution of the heating about the equator. It is also in good agreement with the observed short-time response of the subtropical zonal wind to changes in v_χ discussed in HV90. Namely, the response time between upper-level tropical outflow and SH summer u_ψ enhancements during SOP-1 of the FGGE appeared to be less than 12 hours, which was the temporal resolution of the data.

4. Summary

The purpose of the present investigation has been to substantiate the findings of our earlier observational work through the use of a recent version of the GLA fourth-order GCM. A control integration with full-model physics for the period 6–20 January 1979 was able to reproduce the observed heating and subtropical zonal flow structure over the South Pacific. In one sensitivity run (SST1), the strong heating associated with the SPCZ was gradually reduced in time through the imposition of negative s.s.t. anomalies. The result was a strong reduction in v_χ over the anomaly area. Moreover, the reduced divergent flow in the entrance region of the SPCZ westerly maximum resulted in a strong reduction of the jet. The u_ψ response outside of the subtropical Pacific appeared consistent with the findings of earlier studies that examined the impact of tropical heating on extratropical flows.

Tropical heating was removed from the entire tropical belt in NTLH by ignoring temperature changes due to precipitation processes in the model thermodynamic equation. Here, nearly all tropical divergence was eliminated, and large reductions in the subtropical westerlies in both hemispheres were found at all longitudes. An examination of the response times in NTLH revealed that the divergent circulations reacted to the reduced tropical latent heating within half a day of the beginning of the experiment. As discussed by Paegle and Baker (1983), this indicates that the divergent wind is quickly modified by changes in tropical heating through the propagation of gravity waves. Moreover, changes in the summertime subtropical westerlies occurred in phase with changes in v_χ, in good agreement with the observational findings of HV90. Outside of the SH subtropics, the rotational wind response to the reduced tropical heating was noticeable in 2–3 days.

We realize that the findings here are limited in that they only represent a selected case study. The interactions of divergent and rotational flows in the summertime subtropics may not be as well defined for other time periods as they were in January 1979. However, Vincent *et al.* (1991) have recently examined the SH summer season of

November 1984–April 1985 and found that, over the South Pacific, poleward divergent flow from the tropics was properly positioned to be an important factor in maintaining subtropical wind maxima throughout the season. Additionally, some of our preliminary results from the SH summers of 1986–89 further support the view that the relationship found here occurs frequently and can be identified in routine data sets. As shown by our examination of the momentum budget, however, other forcing terms can also play important roles in maintaining the summer subtropical westerlies.

It would also be interesting to extend the numerical aspects of this study to other cases. The respective roles of gravity- and Rossby-wave propagation were only inferred in the present study. For example, it would be of interest to separate the winds into their Rossby and inertia–gravity modes, perhaps using the technique of Nogues-Paegle and Mo (1988). Finally, as discussed earlier, a large number of integrations with perturbed initial conditions need to be obtained in order to determine the natural variability (with respect to medium-range forecasting) of the version of the GLA GCM used here. This is necessary to document statistically the significance of results from experimental integrations performed with modified model physics. Unfortunately, at this time, we do not possess the resources required to meet this need.

Acknowledgements

The authors want to thank Dr Y. C. Sud for allowing access to the GLA model. Thanks also go to Mr Greg Walker and Mr Bill Whitson for their valuable programming assistance in bringing the model to Purdue, and to the Purdue University Computing Center for providing the necessary computing time. Finally, thanks to Ms Helen Henry for typing the manuscript. This research was sponsored by the National Aeronautics and Space Administration under Contract NAS8-37127 and Grant No. NAG8-836 issued to Dr Dayton G. Vincent, Purdue University.

References

Blackburn, M. 1985 Interpretation of ageostrophic winds and implications for jet stream maintenance. *J. Atmos. Sci.*, **42**, 2604–2620

Daley, R. and Chervin, R. M. 1985 Statistical significance testing in numerical weather prediction. *Mon. Weather Rev.*, **113**, 814–826

Hurrell, J. W. and Vincent, D. G. 1990 Relationship between tropical heating and subtropical westerly maxima in the southern hemisphere during SOP-1, FGGE. *J. Climate*, **3**, 751–768

1991 On the maintenance of short-term subtropical wind maxima in the southern hemisphere during SOP-1, FGGE. *J. Climate*, **4**, in Press

Kalnay, E., Balgovind, R., Chao, W., Edelmann, D., Pfaendtner, J., Takacs, L. and Takano, K. 1983 'Documentation of the GLAS fourth-order general circulation model. Vols. I, II and III.' NASA Tech. Memo 86064, Goddard Space Flight Center, Greenbelt, MD, 20771

Kalnay, E., Mo, K. C. and Paegle, J. 1986 Large-amplitude, short-scale stationary Rossby waves in the southern hemisphere: observations and mechanistic experiments to determine their origin. *J. Atmos. Sci.*, **43**, 252–275

Kiladis, G. N., von Storch, H. and van Loon, H. 1989 Origin of the South Pacific convergence zone. *J. Climate*, **2**, 1185–1195

Lau, K.-M. and Lim, H. 1984 On the dynamics of equatorial forcing of climate teleconnections, *J. Atmos. Sci.*, **41**, 161–176

Matsuno, T. 1966 Numerical integrations of the primitive equations by a simulated backward difference method. *J. Meteorol. Soc. Japan*, **44**, 76–84

Mo, K. C., Pfaendtner, J. P. and Kalnay, E. 1987 A GCM study on the maintenance of the June 1982 blocking in the southern hemisphere. *J. Atmos. Sci.*, **44**, 1123–1142

Newell, R. E., Kidson, J. W., Vincent, D. G. and Boer, G. J. 1972 *The general circulation of the tropical atmosphere and interactions with extratropical latitudes*, Vol. 1. MIT Press, Cambridge, MA 02139

Nogues-Paegle, J. and Mo, K. C. 1988 Transient response of the southern hemisphere subtropical jet to tropical forcing. *J. Atmos. Sci.*, **45**, 1493–1508

Paegle, J. 1978 The transient mass-flow adjustment of heated atmospheric circulations. *J. Atmos. Sci.*, **9**, 1678–1688

Paegle, J. and Baker, W. E. 1983 The influence of the tropics on the prediction of ultralong waves. Part II. Latent heating. *Mon. Weather Rev.*, **111**, 1356–1371

Paegle, J., Paegle, J. N. and Lewis, F. P. 1983 Large scale motions of the tropics in observations and theory. *Pure Appl. Geophys.*, **121**, 947–982

Sadler, J. 1975 'The upper tropospheric circulation over the global tropics.' Tech. Rep. UHMET-75-05, Department of Meteorology, University of Hawaii

Sardeshmukh, P. D. and Hoskins, B. J. 1988 The generation of global rotational flow by steady idealized tropical divergence. *J. Atmos. Sci.*, **45**, 1228–1251

Silva-Dias, P. and Paegle, J. N. 1984 'The partition of energy associated with tropical heat sources.' Presented at the First National Workshop on the Scientific Results of the Global Weather Experiment. Woods Hole, MA, U.S.A., July 9–20, 1984

Somerville, R. C. J., Stone, P. H., Halem, M., Hansen, J. E., Hogan, J. S., Druyan, L. M., Russell, G., Lacis, A. A., Quirk, W. J. and Tenenbaum, J. 1974 The GISS model of the global atmosphere. *J. Atmos. Sci.*, **31**, 84–117

Storch, H., van Loon, H. and Kiladis, G. N. 1988 The Southern Oscillation. Part VIII: Model sensitivity to SST anomalies in the tropical and subtropical regions of the South Pacific convergence zone. *J. Climate*, **1**, 325–331

Sud, Y. C. and Abeles, J. 1980 'Calculation of surface temperature and surface fluxes in the GLAS GCM.' NASA Tech. Memo 82167, Goddard Space Flight Center, Greenbelt, MD, 20771

Sud, Y. C. and Molod, A. 1988 The roles of dry convection, cloud–radiation feedback processes and the influence of recent improvements in the parameterization of convection in the GLA GCM. *Mon. Weather Rev.*, **116**, 2366–2387

Trenberth, K. E. 1986 An assessment of the impact of transient eddies on the zonal flow during a blocking episode using localized Eliassen–Palm flux diagnostics. *J. Atmos. Sci.*, **43**, 2070–2087

Trenberth, K. E. and Chen, S.-C. 1988 Rotational and divergent geopotential components. *J. Atmos. Sci.*, **45**, 2949–2960

Vincent, D. G., Hurrell, J. W., Speth, P., Sperling, T., Fink, A. and Zube, S. 1991 Relationship between intraseasonal oscillation and subtropical wind maxima over the South Pacific Ocean. (submitted to *J. Climate*)

Webster, P. J. and Holton, J. R. 1982 Cross-equatorial response to middle-latitude forcing in a zonally varying basic state. *J. Atmos. Sci.*, **39**, 722–733

Wu, M. L. 1980 The exchange of infrared radiative energy in the troposphere. *J. Geophys. Res.*, **85**, 4084–4090

Zwiers, F. W. and von Storch, H. 1989 Multivariate recurrence analysis. *J. Climate*, **2**, 1538–1553